European Radiology (2019) 29:1841–1847
https://doi.org/10.1007/s00330-018-5730-6

MUSCULOSKELETAL

Comparison of radiomics machine-learning classifiers and feature selection for differentiation of sacral chordoma and sacral giant cell tumour based on 3D computed tomography features

Ping Yin[1] · Ning Mao[1,2] · Chao Zhao[1] · Jiangfen Wu[3] · Chao Sun[1] · Lei Chen[1] · Nan Hong[1]

Received: 20 June 2018 / Revised: 1 August 2018 / Accepted: 28 August 2018 / Published online: 2 October 2018

Abstract

Objective We aimed to identify optimal machine-learning methods for preoperative differentiation of sacral chordoma (SC) and sacral giant cell tumour (SGCT) based on 3D non-enhanced computed tomography (CT) and CT-enhanced (CTE) features.

Methods A total of 95 patients were divided into a training set and a validation set. Three best feature selection methods (Relief, least absolute shrinkage and selection operator (LASSO) and Random Forest (RF)) and three classification methods, including generalised linear models (GLM), support vector machines (SVM) and RF, were compared for their performance in distinguishing SC and SGCT. The performance of the radiomics model was investigated via area under the receiver-operating characteristic curve (AUC) and accuracy (ACC) analysis.

Results The selection method LASSO + classifier GLM had the highest AUC of 0.984 and ACC of 0.897 in the validating set, followed by Relief + GLM (AUC = 0.909, ACC = 0.862) and LASSO + SVM (AUC = 0.900, ACC = 0.862) based on CTE features. For CT features, RF + GLM had the highest AUC of 0.889, while LASSO + GLM achieved a high ACC of 0.793 in the validating set. Regardless of the methods, CTE features significantly outperformed those from CT for the differentiation of SC and SGCT (Z_{AUC} = -3.029, Z_{ACC} = -4.553; $p < 0.05$).

Conclusions Our study demonstrated CTE features performed better than CT features. The selection method LASSO + classifier GLM had the best performance in differentiation of SC and SGCT, which could enhance the application of radiomics methods in sacral tumours.

Key Points

- *Sacral chordoma and sacral giant cell tumour are the two most common primary tumours of the sacrum with many common clinical and imaging characteristics.*
- *A radiomics model helps clinicians to identify the histology of a sacral tumour.*
- *CTE features should be preferred.*

Keywords Sacrum · Bone neoplasms · Algorithms · Machine learning

✉ Nan Hong
hongnan@bjmu.edu.cn

[1] Department of Radiology, Peking University People's Hospital, 11 Xizhimen Nandajie, Xicheng District, Beijing 100044, People's Republic of China

[2] Department of Radiology, Qindao University Medical College Affiliated Yantai Yuhuangding Hospital, Yantai, Shandong, People's Republic of China

[3] GE Healthcare, Shanghai, People's Republic of China

Abbreviations

ACC	Accuracy
AUC	Area under the receiver-operating characteristic curve
CT	Computed tomography
CTE	Computed tomography enhanced
FOV	Field of view
GLM	Generalised linear models
ICC	Intra- and interclass correlation coefficients
LASSO	Least absolute shrinkage and selection operator

MDCT	Multi-detector row CT
PACS	Picture archiving and communication system
RF	Random Forest
ROIs	Regions of interest
SC	Sacral chordoma
SGCT	Sacral giant cell tumour
SVM	Support vector machines

Introduction

Sacral tumours are rare, but all components of the sacrum (bone, cartilage, bone marrow, notochord remnants, etc.) can give rise to benign or malignant tumours [1–3]. Sacral chordoma (SC) and sacral giant cell tumour (SGCT) are the two most common primary tumours of the sacrum, accounting for about 40% and 13% of all primary sacral tumours, respectively [4]. They share many common clinical and imaging characteristics, however, the treatment approaches for SC and SGCT are quite different. Due to the high recurrence rate of SC, lumbar resection of tumour is the preferred method for reducing the local recurrence rate. The SGCT is located in the upper sacrum and represents a benign tumour; intralesional curettage is commonly performed. The greatest challenge and key point in the treatment of SGCT is intraoperative haemorrhage, because the rich blood supply in this area often causes more haemorrhage during the operation [3–5]. Therefore, accurate preoperative diagnosis is of great importance in guiding the clinical approach.

A computed tomography (CT) scan is the first choice of imaging method to delineate sacral tumours. A CT scan and CT-enhanced (CTE) scan, especially thin-slice helical acquisition with two-dimensional (2D) and three-dimensional (3D) reconstructions, are superior in showing bony details such as special calcification, bone residues and invasion of the spinal canal [4]. CTE can also improve the discrimination of cystic or necrotic tissue shown as reduced attenuation areas, while vascularised tumour areas appear as brighter enhanced heterogeneous areas than other areas [6]. In clinical practice, both SC and SGCT are rarely diagnosed at the early stage due to rare or nonspecific symptoms, but rather in a late stage [7]. The preoperative identification of SC and SGCT is difficult for radiologists when they appear as heterogeneous masses mixed with necrosis, haemorrhage, calcification or residual bone on CT. Biopsy is the most common way of classifying tumour histology before surgery, but it is invasive and only evaluates a small sample, which may produce complications, sampling error and poor efficiency [8].

Radiomics is a new emerging non-invasive method that extracts high-dimensional sets of imaging features for building appropriate models for assessing the ability of clinical diagnosis, prognosis and therapeutic effect, based on characterising intratumoural heterogeneity [9–15]. CT radiomics analysis has shown promise in lesion characterisation, pretreatment tumour assessment and response evaluation for many tumour types [16]. 3D CT radiomics features were calculated and extracted from the whole layers of tumour lesion in CT images, and have been explored in many studies [17–19]. CTE features can reflect blood vessels and blood flow of the tumour that correlate with the metabolic activity of the tumour [20]. Most published studies have assessed the predictive abilities of radiomics features; only a few recent studies have shown that the performance of a radiomics model can be greatly influenced by different feature selections and classification approaches [21–23]. It was, however, still unknown whether the feature selection and classification methods affect the performance of radiomics features for distinguishing sacral tumour.

The objective of this study was to identify optimal machine-learning methods for the preoperative differentiation of SC and SGCT based on 3D CT and CTE features. We investigated nine cross-combinations of three commonly used feature selection methods and three classification methods in terms of their performance in distinguishing SC and SGCT, which may enhance the precision of preoperative diagnosis and personalised treatment.

Material and methods

Patient cohort and image acquisition

Subsequent to approval from the local ethics committee of our hospital, a database of 143 patients from January 2006 to October 2017 with pathologically confirmed sacrum tumour (87 SCs and 56 SGCTs) before therapy were retrospectively analysed. All patients met the following inclusion criteria: had a sacrum tumour mentioned in preoperative CT and CTE reports; CT and CTE images were complete; pathology reports confirmed SC or SGCT. Exclusion criteria: images with poor quality including obvious artefacts; patients without enhanced images. Finally, 95 patients, consisting of 53 SCs and 42 SGCTs, were analysed.

All CT and CTE images were collected from the picture archiving and communication system (PACS) of our hospital. For plain CT scans, images were acquired on each patient using multidetector row CT (MDCT) systems (Philips iCT 256, Philips Medical System), with the following acquisition parameters: 120 kV, 685 mAs, 256 × 0.625 collimator configuration, slice thickness = 5 mm, matrix = 320 × 224 mm, field of view (FOV) = 350 × 350 mm. CTE was performed after a 70-s delay following intravenous administration of 1.5 ml/kg of iodinated contrast medium (iopamidol injection, 370 mg I/ml, Bracco Sine Pharma) and 20 ml of saline at a rate of 2.5 ml/s with an automatic pump injector (Ulrich CT Plus 150, Ulrich Medical). The CT images were reconstructed with a standard kernel.

Tumour segmentation

We exported all CT, CTE Digital Imaging and Communications in Medicine images from PACS for tumour segmentation. The itk-SNAP software (www.itk-snap.org) was used for manual segmentation. All regions of interest (ROIs) were handcrafted on both CT and CTE images on each slice by two musculoskeletal radiologists who had more than 10 years of experience. Intra- and interclass correlation coefficients (ICCs) were used to evaluate inter-observer and intra-observer reproducibility of ROI delineation. We initially chose 30 random images for ROI segmentation by two radiologists independently. To assess intra-observer reproducibility, each reader repeated the same manual procedure 1 week later. An ICC greater than 0.75 was considered good agreement [24] (Fig. 1).

Radiomics feature selection methods

A total of 770 radiomics features of each patient were extracted from all CT and CTE images based on Artificial Intelligence Kit version1.0.3 (GE Healthcare). The radiomics features were divided into three groups: tumour intensity, morphology and texture features [22]. Three selection methods were validated in this study: Relief [21], least absolute shrinkage and selection operator (LASSO) [25, 26], and Random Forest (RF) [23]. We chose these methods mainly because of their popularity and efficiency in the literature [21–26]. The differentiation of performance of selection methods was evaluated in the all-patients sample.

Classifiers

For features classification, the following three classifiers with high stability were investigated: support vector machines (SVM), generalised linear models (GLM) and RF. Classifiers were trained using the repeated tenfold cross-validation method in the training set and the differentiation performance was evaluated with a validating set.

Validation of the radiomics model

The stability of feature selection and classification methods was assessed using the area under the receiver-operating characteristic curve (AUC) and accuracy (ACC). AUC ≥ 0.894 (upper quartile of AUC value) and ACC ≥ 0.854 (upper quartile of ACC value) in the validating set were considered as highly accurate classification performance.

Statistical analysis

The statistical analyses were performed with R software (R Core Team) version 3.4.3. A Mann-Whitney U test was performed using SPSS version 17 software (SPSS, Inc.) to compare the difference in clinical and imaging data between the groups. A comparison of the composition ratio was checked by the Chi-square test. All statistical tests were two-sided, and p-values of < 0.05 were considered statistically significant.

Results

Clinical characteristics of the patients

In total, 95 eligible sacrum tumour patients (54 males, 41 females; mean age of 47.9 ± 17.1 years, range 17–79) were retrospectively analysed. Sixty-six sacrum tumour patients (37 SCs, 29 SGCTs) were assigned to a training set, and 29 patients to a validating set (16 SCs, 13 SGCTs) according to a ratio of 7:3. No significant differences were found between the training and validating sets in terms of age, sex, tumour

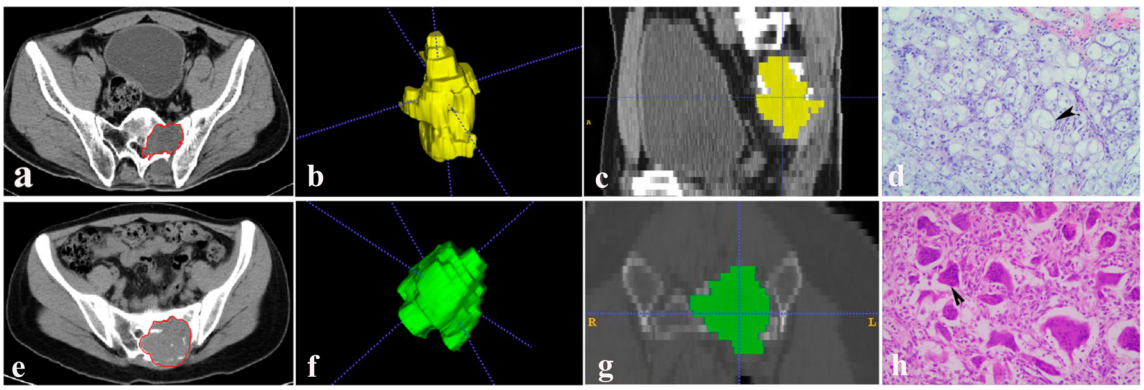

Fig. 1 Segmentation of tumours. **a-d** SC in a 48-year-old man. **a** Axial CT scan (soft tissue window) showing the irregular margin of tumour, (**b**) 3D ROI, (**c**) sagittal CTE images, (**d**) pathological image showing oval vacuolated epithelial cells (black arrowhead), hyalinised extracellular matrix with extensive myxoid regions and fibrous septa. **e-h** SGCT in a 23-year-old woman. **e** Axial CT scan (soft tissue window) showing the irregular margin of tumour and residual bone, (**f**) 3D ROI, (**g**) coronal CTE images presented an oval morphology and bone destruction of the tumour (green), (**h**) pathological image showing lots of polynuclear giant cells (black arrowhead) and mononuclear stromal cells

Table 1 Clinical characteristics of patients in the training and validation sets

	Training set	Validation set	χ^2/ Z value	*p*-value
Sex				
Male	38	16	$\chi^2 = 0.013$	0.909
Female	28	13	$\chi^2 = 0.019$	0.891
Age (y)				
Median (P25~P75)	50.0 (34.0~62.0)	44.0 (33.5~55.0)	Z = -0.703	0.482
Location				
Upper sacrum (S1-2)	29	12	$\chi^2 = 0.022$	0.883
Lower sacrum (S3-5)	20	11	$\chi^2 = 0.265$	0.607
Whole sacrum (S1-5)	17	6	$\chi^2 = 0.175$	0.676
Size (cm)				
Median (P25~P75)	8.45 (6.83~11.78)	8.80 (6.65~9.95)	Z = -0.044	0.965
Histology				
SC	37	16	$\chi^2 = 0.002$	0.966
SGCT	29	13	$\chi^2 = 0.002$	0.960

SC sacral chordoma, *SGCT* sacral giant cell tumour

location, tumour size and histology ($p > 0.05$) (Table 1). Tumour location in the sacrum was defined as upper (S1-2), lower (S3-5) and whole sacral location (S1-5).

Performance of feature selection methods and classifiers

Satisfactory inter-observer (ICC, range 0.812–0.934) and intra-observer (ICC, 0.863–0.986) reproducibility of manual delineation was achieved. A total of 770 radiomics features of each patient were extracted from CT (385 features) and CTE (385 features).

For CT features, the selection method RF + classifier GLM had the highest AUC of 0.889, which declined to LASSO + GLM and Relief + SVM, while LASSO + GLM also achieved the highest ACC of 0.793 in the validating set. For CTE features, the selection method LASSO + classifier GLM had the highest AUC of 0.984 in the validating set, followed by Relief + GLM (AUC = 0.909) and RF + RF (AUC = 0.904) (Table 2, Fig. 2).

For both CT and CTE features, the selection method LASSO + classifier GLM had the highest ACC, while the selection method RF + classifier SVM also achieved a high ACC of 0.897 based on CTE features (Table 3, Fig. 3).

No significant difference was found either among three feature selection methods or three classification methods for the performance of feature selection and classifiers ($p > 0.05$).

Stability and differentiation values of the radiomics model

In the training set, the radiomics feature derived from CTE images yielded the highest AUC of 1 and ACC of 0.955, which is higher than those of the CT images (AUC = 1; ACC = 0.879).

In the validating set, a similar result was found: the radiomics feature derived from CTE images yielded the highest AUC of 0.984 and ACC of 0.897, while that from CT images yielded an AUC of 0.889 and ACC of 0.793.

For the whole cross-combination methods in the validating set, features extracted from CTE images had significantly higher AUC and ACC values than those of CT images in terms of differentiation of SC and SGCT ($Z_{AUC} = -3.029$, $Z_{ACC} = -4.553$; $p < 0.05$).

Considering the AUC and ACC together, the best performance of differential diagnosis based on the selection method

Table 2 The mean AUC of the cross-combination methods

AUC	GLM	SVM	RF
CT features			
ReliefF	0.834 (0.813)	0.905 (0.864)	1 (0.639)
LASSO	0.850 (0.865)	0.862 (0.841)	1 (0.786)
RF	0.867 (0.889)	0.957 (0.798)	1 (0.673)
CTE features			
ReliefF	0.981 (0.909)	0.985 (0.894)	1 (0.889)
LASSO	0.984 (0.984)	0.979 (0.900)	1 (0.875)
RF	0.973 (0.889)	0.986 (0.894)	1 (0.904)

The AUC of the cross-combination methods based on CT and CTE features are showed in the training set (no brackets) and the validating set (in brackets)

AUC area under the receiver-operating characteristic curve, *GLM* generalised linear models, *SVM* support vector machines, *RF* Random Forest, *CT* computed tomography, *CTE* CT-enhanced, *LASSO* least absolute shrinkage and selection operator

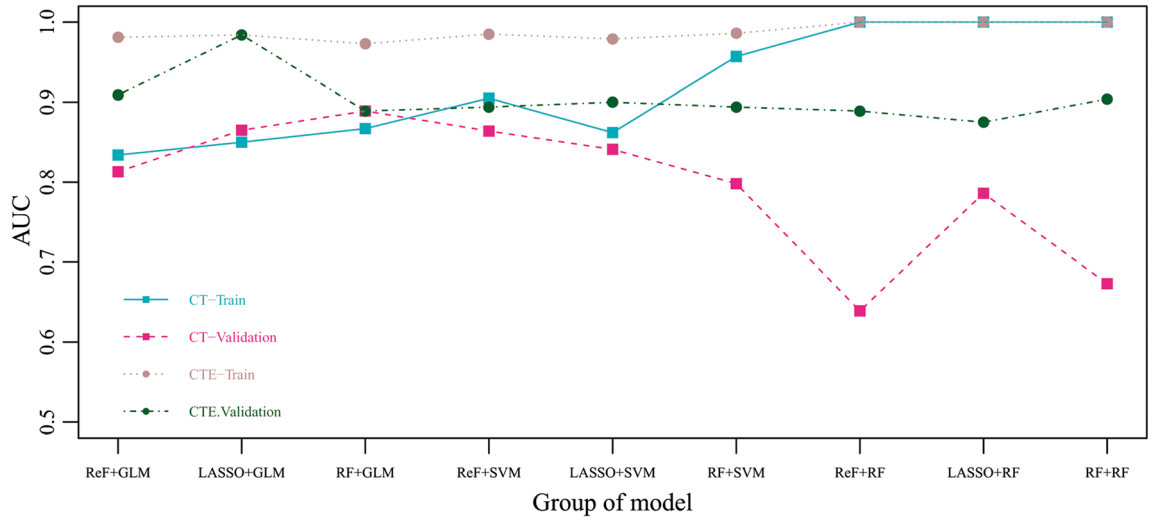

Fig. 2 Scatterplots depicting the AUC of the cross-combination methods based on CT and CTE features. The selection method LASSO + classifier GLM had the highest AUC in the validation set. CTE features had a higher AUC than CT

LASSO + classifier GLM from CTE features reached the highest AUC of 0.984 and ACC of 0.897 in the validating set, followed by Relief + GLM (AUC = 0.909, ACC = 0.862) and LASSO + SVM (AUC = 0.900, ACC = 0.862).

Discussion

In the current study, we developed and validated a 3D CT and CTE-based radiomics model as a novel approach to differentiate SC and SGCT, providing an optimal method to improve decision-support in sacral tumour at low cost. The highest performance was found in the combination of the selection method LASSO + classifier GLM. Furthermore, radiomics features extracted from CTE images significantly outperformed CT images in terms of differentiation of SC and SGCT.

Table 3 The ACC of the cross-combination methods

ACC	GLM	SVM	RF
CT features			
ReliefF	0.803 (0.724)	0.789 (0.621)	0.773 (0.690)
LASSO	0.742 (0.793)	0.833 (0.759)	0.727 (0.759)
RF	0.758 (0.759)	0.879 (0.690)	0.788 (0.621)
CTE features			
ReliefF	0.924 (0.862)	0.924 (0.862)	0.879 (0.793)
LASSO	0.955 (0.897)	0.924 (0.862)	0.833 (0.793)
RF	0.924 (0.793)	0.924 (0.897)	0.864 (0.828)

The AUC of the cross-combination methods based on CT and CTE features are showed in the training set (no brackets) and the validating set (in brackets)

AUC area under the receiver-operating characteristic curve, *GLM* generalised linear models, *SVM* support vector machines, *RF* Random Forest, *CT* computed tomography, *CTE* CT-enhanced, *LASSO* least absolute shrinkage and selection operator

To improve the stability and classification performance of the radiomics model, Hawkins et al compared four different feature selection and classification methods for CT-based survival prediction of lung cancer [27]. Parmar et al first evaluated 14 feature selection methods and 12 classification methods to predict overall survival of lung cancer patients [22], then chose 13 feature selection methods and 11 classification methods to predict overall survival of head and neck cancer patients [28]. However, these previous studies compared different feature selection and classification methods, respectively; only Zhang et al compared 54 cross-combinations of six feature selection methods and nine classification methods for prediction of local and distant failure in advanced nasopharyngeal carcinoma [23]. In addition, these studies were mainly focused on the prediction of clinical outcomes, and only Wu et al compared 24 feature selection and three classification methods for the prediction of lung cancer histology (adenocarcinoma and squamous cell carcinoma) [21]. Unlike previous studies, we investigated nine cross-combinations of three feature selection methods and three classification methods because of they have commonly been used and achieved higher performance in previous studies. Furthermore, we compared their performance for differentiating SC and SGCT based on CT and CTE images, respectively. As far as we know, this is the first study to investigate the differentiation of SC and SGCT using 3D CT features.

Considering the AUC and ACC together, the selection method LASSO + classifier GLM, Relief + GLM and RF + SVM had a comparatively higher performance in distinguishing SC and SGCT. For the performance of three feature selection methods, LASSO achieved relatively higher AUC and ACC than RF and Relief. For the performance of three classification methods, SVM performed better than GLM and RF. Nevertheless, no

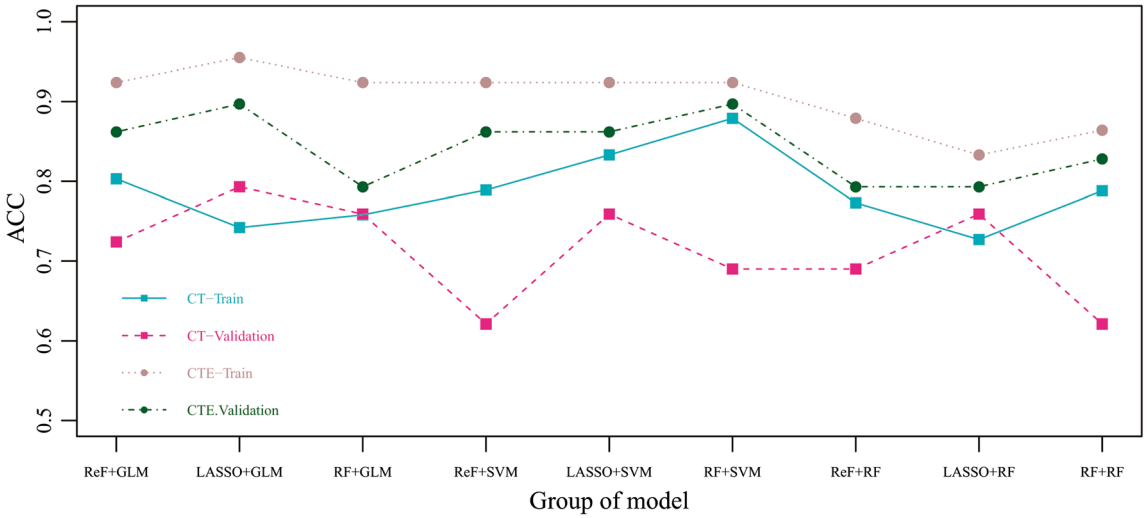

Fig. 3 Scatterplots depicting the ACC of the cross-combination methods based on CT and CTE features. The selection method LASSO + classifier GLM had the highest ACC in both the training set and the validation set

significant difference was found either among three feature selection methods or three classification methods. LASSO is an outstanding method for feature selection by retaining the good features of both subset selection and ridge regression [24]. It is suitable for analysing large sets of radiomics features with a relatively small sample size, and it is designed to avoid overfitting [29]. GLM is a classical linear classification method; Parmar et al found GLM had the highest prognostic performance in predicting overall survival of head and neck cancer among 11 classification methods [28]. Relief can detect context information among features and thus more accurately deals with situations where dependencies are present, but is unable to detect redundant features [21, 30]. SVM is often reported to provide better classification because it obtains optimal results using available information and shows better generalisation ability on the unseen data [31]. The RF is quite an efficient model-free method both in variable selection and in classification, and consists of a collection of decision trees [21, 23, 32]. It is robust to noises and outliers, and can handle high-dimension spaces rapidly, but has an over-fitting problem [33, 34]. Our results demonstrated that LASSO + classifier GLM had the best performance in both CT and CTE features, indicating feature selection LASSO + classifier GLM is a preferred and stable machine-learning method for the differentiation of SC and SGCT.

In this study, we used the 3D CT and CTE features to build the model and achieved a high performance in differentiating SC and SGCT. Our results indicated that CTE features can provide more useful information for the identification of SC and SGCT than CT features.

There are some limitations of this study. First, images were acquired over the course of several years and all of our imaging data come from a single centre; a multicentre study with a large sample size is needed for further study. Second, we only compared three commonly used feature selection methods and three classification methods in terms of their performance of distinguishing SC and SGCT; we did not know the results of other machine-learning methods. Lastly, the model can be enhanced if we incorporate more clinical and genetic features in a future study.

Conclusions

In summary, our radiomics study identified optimal machine-learning methods for the preoperative differentiation of SC and SGCT, which could enhance the application of radiomics methods in the precision of diagnosis of sacral tumour.

Funding The authors state that this work has not received any funding.

Compliance with ethical standards

Guarantor The scientific guarantor of this publication is Jiangfen Wu.

Conflict of interest The authors of this article declare no relationships with any companies whose products or services may be related to the subject matter of the article.

Statistics and biometry One of the authors has significant statistical expertise.

Informed consent Written informed consent was waived by the Institutional Review Board.

Ethical approval Institutional Review Board approval was obtained.

Methodology
- Retrospective
- Diagnostic or prognostic study
- Performed at one institution

References

1. Thornton E, Krajewski KM, O'Regan KN, Giardino AA, Jagannathan JP, Ramaiya N (2012) Imaging features of primary and secondary malignant tumours of the sacrum. Br J Radiol 85(1011):279–286
2. Gerber S, Ollivier L, Leclère J et al (2008) Imaging of sacral tumours. Skeletal Radiol 37(4):277–289
3. Ji T, Guo W, Yang R, Tang X, Wang Y, Huang L (2017) What are the conditional survival and functional outcomes after surgical treatment of 115 patients with sacral chordoma? Clin Orthop Relat Res 475(3):620–630
4. Si MJ, Wang CS, Ding XY et al (2013) Differentiation of primary chordoma, giant cell tumor and schwannoma of the sacrum by CT and MRI. Eur J Radiol 82(12):2309–2315
5. Jamshidi K, Bagherifard A, Mirzaei A, Bahrabadi M (2017) Giant cell tumor of the sacrum: series of 19 patients and review of the literature. Arch Bone Jt Surg 5(6):443–450
6. Avanzo M, Stancanello J, El Naqa I (2017) Beyond imaging: the promise of radiomics. Phys Med 38:122–139
7. Ruosi C, Colella G, Di Donato SL, Granata F, Di Salvatore MG, Fazioli F (2015) Surgical treatment of sacral chordoma: survival and prognostic factors. Eur Spine J 24(Suppl 7):912–917
8. Vallières M, Freeman CR, Skamene SR, El Naqa I (2015) A radiomics model from joint FDG-PET and MRI texture features for the prediction of lung metastases in soft-tissue sarcomas of the extremities. Phys Med Biol 60:5471–5496
9. Shen C, Liu Z, Guan M et al (2017) 2D and 3D CT radiomics features prognostic performance comparison in non-small cell lung cancer. Transl Oncol 10(6):886–894
10. Bowen SR, Yuh WTC, Hippe DS et al (2018) Tumor radiomic heterogeneity: multiparametric functional imaging to characterize variability and predict response following cervical cancer radiation therapy. J Magn Reson Imaging 47(5):1388–1396
11. Larue RT, Defraene G, De Ruysscher D, Lambin P, van Elmpt W (2017) Quantitative radiomics studies for tissue characterization: a review of technology and methodological procedures. Br J Radiol 90(1070):20160665
12. Yip SS, Aerts HJ (2016) Applications and limitations of radiomics. Phys Med Biol 61(13):R150–R166
13. Lambin P, Leijenaar RTH, Deist TM et al (2017) Radiomics: the bridge between medical imaging and personalized medicine. Nat Rev Clin Oncol 14(12):749–762
14. Kickingereder P, Burth S, Wick A et al (2016) Radiomic profiling of glioblastoma: identifying an imaging predictor of patient survival with improved performance over established clinical and radiologic risk models. Radiology 280(3):880–889
15. Liu J, Mao Y, Li Z et al (2016) Use of texture analysis based on contrast-enhanced MRI to predict treatment response to chemoradiotherapy in nasopharyngeal carcinoma. J Magn Reson Imaging 44:445–455
16. Lubner MG, Smith AD, Sandrasegaran K, Sahani DV, Pickhardt PJ (2017) CT texture analysis: definitions, applications, biologic correlates, and challenges. Radiographics 37(5):1483–1503
17. Cha KH, Hadjiiski L, Chan HP et al (2017) Bladder cancer treatment response assessment in CT using radiomics with deep-learning. Sci Rep 7(1):8738
18. Pota M, Scalco E, Sanguineti G et al (2017) Early prediction of radiotherapy-induced parotid shrinkage and toxicity based on CT radiomics and fuzzy classification. Artif Intell Med 81:41–53
19. Bashir U, Azad G, Siddique MM et al (2017) The effects of segmentation algorithms on the measurement of 18F-FDG PET texture parameters in non-small cell lung cancer. EJNMMI Res 7(1):60
20. Tixier F, Groves AM, Goh V et al (2014) Correlation of intra-tumor (18)F-FDG uptake heterogeneity indices with perfusion CT derived parameters in colorectal cancer. PLoS One 9:e99567
21. Wu W, Parmar C, Grossmann P et al (2016) Exploratory study to identify radiomics classifiers for lung cancer histology. Front Oncol 6:71
22. Parmar C, Grossmann P, Bussink J, Lambin P, Aerts HJ (2015) Machine learning methods for quantitative radiomic biomarkers. Sci Rep 5:13087
23. Zhang B, He X, Ouyang F et al (2017) Radiomic machine-learning classifiers for prognostic biomarkers of advanced nasopharyngeal carcinoma. Cancer Lett 403:21–27
24. Wu S, Zheng J, Li Y et al (2017) A radiomics nomogram for the preoperative prediction of lymph node metastasis in bladder cancer. Clin Cancer Res 23(22):6904–6911
25. Zhu X, Dong D, Chen Z et al (2018) Radiomic signature as a diagnostic factor for histologic subtype classification of non-small cell lung cancer. Eur Radiol. https://doi.org/10.1007/s00330-017-5221-1
26. Sun Y, Hu P, Wang J et al (2018) Radiomic features of pretreatment MRI could identify T stage in patients with rectal cancer: Preliminary findings. J Magn Reson Imaging. https://doi.org/10.1002/jmri.25969
27. Hawkins SH, Korecki JN, Balagurunathan Y et al (2014) Predicting outcomes of nonsmall cell lung cancer using CT image features. IEEE Access 2:1418–1426
28. Parmar C, Grossmann P, Rietveld D, Rietbergen MM, Lambin P, Aerts HJ (2015) Radiomic machine-learning classifiers for prognostic biomarkers of head and neck cancer. Front Oncol 5:272
29. Zhang B, Tian J, Dong D et al (2017) Radiomics features of multiparametric MRI as novel prognostic factors in advanced nasopharyngeal carcinoma. Clin Cancer Res 23(15):4259–4269
30. Yuan M, Zhang YD, Pu XH et al (2017) Comparison of a radiomic biomarker with volumetric analysis for decoding tumour phenotypes of lung adenocarcinoma with different disease-specific survival. Eur Radiol 27(11):4857–4865
31. Asl BM, Setarehdan SK, Mohebbi M (2008) Support vector machine-based arrhythmia classification using reduced features of heart rate variability signal. Artif Intell Med 44(1):51–64
32. Parekh V, Jacobs MA (2016) Radiomics: a new application from established techniques. Expert Rev Precis Med Drug Dev 1(2):207–226
33. Breiman L (2001) Random forests. Mach Learn 45(1):5–32
34. Fernández-Delgado M, Cernadas E, Barro S, Amorim D (2014) Do we need hundreds of classifiers to solve real world classification problems? J Mach Learn Res:3133-3181